Unification of coherence and quantum correlations in tripartite systems

Dong-Dong Dong, Geng-Biao Wei, Xue-Ke Song,* Dong Wang,† and Liu Ye
School of Physics and Optoelectronics Engineering, Anhui University, Hefei 230601, People's Republic of China

(Received 17 May 2022; revised 16 August 2022; accepted 30 September 2022; published 13 October 2022)

In quantum resource theories (QRTs), evidence of intrinsic connections between coherence and quantum correlations, including Bell nonlocality, entanglement, quantum steering, and so on, exists. However, building these relationships is a vital yet challenging task in multipartite quantum systems. Here, we focus on a unified framework of interpreting the interconversions among coherence and different quantum correlations in tripartite systems. In particular, an exact relation between the generalized geometric measure and the genuinely multipartite concurrence is derived for tripartite entanglement states. Then we obtain the trade-off relation between the first-order coherence and the genuine tripartite entanglement by the genuinely multipartite concurrence and concurrence fill. Furthermore, the trade-off relation between the maximum steering inequality violation and concurrence fill for arbitrary three-qubit states is found. In addition, we investigate the close relation between the maximum steering inequality violation and the first-order coherence. The results show that coherence and quantum correlations are intrinsically related and can be converted to one another in the framework of QRTs.

DOI: 10.1103/PhysRevA.106.042415

I. INTRODUCTION

Coherence and quantum correlations, as two related properties of a compound system, are known as vital physical resources in quantum information processing from the perspective of quantum resource theories (QRTs) [1–3]. Coherence is an essential concept to show the traits of a stream of photons [4], and it characterizes the interference capability of the compound system. It plays a key role in various quantum algorithms and quantum communication protocols [5,6]. Also it is the main reason why quantum tasks can be realized faster than classical ones [7]. On the other hand, quantum correlations, as the description of interdependence among subsystems, fall into several categories, such as Bell nonlocality [8], entanglement [9–17], and steering [18–26]. Since both of them can be quantified and characterized by the QRTs, it is reasonable to investigate whether they can be quantitatively converted [27–35].

In recent years, many efforts have been made to study the relation between coherence and quantum correlations [36–41]. In 2013, Kagalwala *et al.* experimentally found a complementary relation between first-order coherence and Bell nonlocality in the bipartite pure-state case [36]. In 2015, this finding was generalized to the mixed-state case by Svozilík *et al.* [37]. They also investigated the conservation between first-order coherence and the degree of entanglement by global unitary transformations, which was verified via an experiment by Černoch *et al.* in 2018 [39]. Similarly, another complementary relation between first-order coherence and entanglement was found for two-qubit states in 2019 [40]. In addition, quantum steering is also a quantum correlation that lies between Bell nonlocality and entanglement [42]. Steerable states have been shown to have many potential applications in randomness generation [43], subchannel discrimination [44], quantum information processing [45], and one-sided device-independent processing in quantum key distributions [46]. Recently, the relationship between first-order coherence and the maximum violation of the three-setting linear-steering inequality was studied in a two-qubit system [47]. It was later verified experimentally by preparing biphoton polarization-entangled states in an all-optical setup in the same year [48]. These studies reveal that the coherence and the different measures of quantum correlations can be transformed from one another by unitary operations, which is helpful for exploring the fundamental connections among these quantum resources.

On the other hand, many indications show that different quantum correlations are intrinsically connected [49–53]. For example, in 2020, the shareability of three-setting linear steering and its relationship with bipartite or tripartite entanglement of three-qubit states were investigated by Paul and Mukherjee [52]. More recently, Dai *et al.* presented a further study on the complementary relations between tripartite entanglement and the reduced bipartite steering for three-qubit states in 2022 [53]. However, it is worth noting that most of the related studies concern two-qubit systems. Little attention has been paid to the whole entangled multipartite system. In fact, investigations of the relationship between coherence and different quantum correlations in tripartite systems are important for understanding information transfer and flow in the framework of QRTs.

In this paper, we establish a unification of coherence and quantum correlations, including quantum entanglement and quantum steering, in arbitrary tripartite entanglement states. First, we establish an exact functional relation between the generalized geometric measure (GGM) and the genuinely

*songxk@ahu.edu.cn
†dwang@ahu.edu.cn

multipartite concurrence (GMC) for three-qubit pure states, although the relationship is restricted by an inequality in the mixed-state scenario. Then, the trade-off relation between the first-order coherence and the genuine tripartite entanglement is found, where the measures of entanglement are quantified by the GMC and a recently defined faithful tripartite entanglement, concurrence fill [17]. In addition, we find that a trade-off relation between the maximum steering inequality violation and concurrence fill exists. Moreover, we present the close relation between the maximum steering inequality violation and first-order coherence. Note that the boundary states of all the above relations consist of the three states: $|\psi\rangle_\alpha$, $|\psi\rangle_m$, and $|\psi\rangle_\theta$. These relations provide evidence that coherence and different measures of quantum correlations are, indeed, interconnected and can be converted to one another.

This paper is organized as follows: In Sec. II, we briefly review some measures of coherence and quantum correlations. In Sec. III, we give the relation between the GGM and GMC. In Sec. IV, we present the trade-off relations between the genuine tripartite entanglement and the first-order coherence. We study the trade-off relation between the maximum steering inequality violation and concurrence fill in Sec. V. The close relationship between the maximum steering inequality violation and first-order coherence is derived in Sec. VI. A summary is provided in Sec. VII.

II. PRELIMINARIES

Here, we give a brief overview of coherence and different measures of quantum correlations, including quantum entanglement and the steering inequality. We use the GGM, GMC, and concurrence fill, which have already been generated and verified by experiments [54–56], as the measures of genuine tripartite entanglement. The coherence and steering inequality are quantified by first-order coherence and the three-setting linear-steering inequality, respectively.

A. GGM

The GGM, as a generalization of the measure defined by Wei and Goldbart [14], is based on the geometric distance between the n-partite state $|\psi\rangle$ and the set of all multiparty states $|\varphi\rangle$ that are not genuinely entangled. That is [11],

$$\mathcal{G}(|\psi\rangle) = 1 - \max_{|\varphi\rangle} |\langle\varphi \mid \psi\rangle|^2, \tag{1}$$

where the maximization is done over all separable states $|\varphi\rangle$. An equivalent mathematical expression of the GGM is given by

$$\mathcal{G}(|\psi\rangle)=1-\max\left\{\varepsilon_{I:L}^2 | I\cup L=\{1,2,\dots,n\}, I\cap L=\emptyset\right\}, \tag{2}$$

where $\varepsilon_{I:L}$ is the maximal Schmidt coefficient in the $I:L$ split of the state $|\psi\rangle$. For the arbitrary pure states, $\varepsilon_{I:L}^2$ are equal to the corresponding eigenvalues of the reduced density matrices ρ_I as well as ρ_L.

The GGM is generalized to mixed states ρ via the convex roof construction [12]

$$\mathcal{G}(\rho) = \inf_{\{p_i,|\psi_i\rangle\}} \sum_i p_i \mathcal{G}(|\psi_i\rangle), \tag{3}$$

where the infimum is over all feasible decompositions $\rho = \sum_i p_i|\psi_i\rangle\langle\psi_i|$.

B. GMC

For multipartite pure states, Ma *et al.* [15] defined the GMC satisfying the necessary conditions for being a multipartite entanglement measure. It is related to the entanglement of the minimum bipartite linear entropies, instead of von Neumann entropies. For an n-partite pure state $|\psi\rangle \in \mathcal{H}_1 \otimes \mathcal{H}_2 \otimes \cdots \otimes \mathcal{H}_n$ with $\dim(\mathcal{H}_i) = d_i$, $i = 1, 2, \dots, n$, the GMC is defined as

$$\mathcal{C}(|\psi\rangle) = \min_{\mu_i} \sqrt{2\left[1 - \mathrm{Tr}\left(\rho_{A_{\mu_i}}^2\right)\right]}, \tag{4}$$

where μ_i donates the elements in the set of all feasible bipartitions $\{A_i|B_i\}$. The GMC is also generalized to mixed states ρ via the convex roof construction

$$\mathcal{C}(\rho) = \inf_{\{p_i,|\psi_i\rangle\}} \sum_i p_i \mathcal{C}(|\psi_i\rangle). \tag{5}$$

C. Concurrence fill

For tripartite entanglement states, concurrence fill is introduced as a faithfully genuine entanglement measure based on the area of an alleged concurrence triangle [17]. In the proposal, the lengths of the three sides are set equal to the squares of the three bipartite concurrences. From Heron's formula for triangle area, the concurrence fill can be defined as

$$\mathcal{F}(|\psi\rangle) = \left[\tfrac{16}{3} Q\left(Q - C_{A(BC)}^2\right)\left(Q - C_{B(AC)}^2\right)\left(Q - C_{C(AB)}^2\right)\right]^{1/4}, \tag{6}$$

where

$$Q = \tfrac{1}{2}\left(C_{A(BC)}^2 + C_{B(AC)}^2 + C_{C(AB)}^2\right). \tag{7}$$

Q is the half perimeter, which is equivalent to the global entanglement [57,58]. The coefficient 16/3 guarantees the normalizing condition that $0 \leqslant \mathcal{F}_{123} \leqslant 1$, and the extra square root exceeding Heron's formula ensures local monotonicity under the local quantum operations assisted by classical communications. $C_{i(jk)}$ can be calculated as follows [59]:

$$C_{i(jk)} = 2\sqrt{\det \rho_i}, \tag{8}$$

where $i, j, k \in \{A, B, C\}$, $i \neq j \neq k$, and ρ_i is the reduced density matrices of the quantum state ρ_{ABC}. It can be found that $0 \leqslant C_{i(jk)} \leqslant 1$. Concurrence fill can detect the difference between entanglements of some states, while other genuine multipartite entanglement measures cannot. In particular, for three-qubit systems, the GMC is equal to the square root of the shortest side length of the concurrence triangle.

D. First-order coherence

For the three-qubit arbitrary state ρ_{ABC}, the first-order coherence for each subsystem A, B, or C is defined by its purity [4]

$$\mathcal{D}(\rho_i) = \sqrt{2\,\mathrm{Tr}\left(\rho_i^2\right) - 1}, \tag{9}$$

where $i \in \{A, B, C\}$. When all subsystems are regarded independently, the first-order coherence for the state ρ_{ABC} is given by [37]

$$\mathcal{D}(\rho_{ABC}) = \sqrt{\frac{\mathcal{D}(\rho_A)^2 + \mathcal{D}(\rho_B)^2 + \mathcal{D}(\rho_C)^2}{3}}, \tag{10}$$

where $0 \leqslant \mathcal{D}(\rho_{ABC}) \leqslant 1$. Note that the first-order coherence is independent of the selection of the reference basis.

E. The three-setting linear-steering inequality violation

Cavalcanti *et al.* [19] formulated the following linear-steering inequalities to verify whether a bipartite state is steerable from Alice to Bob when both of them are able to operate n dichotomic measurements on their own subsystems:

$$F_n(\rho_{AB}, \mu) = \frac{1}{\sqrt{n}}\left|\sum_{k=1}^{n} \langle A_k \otimes B_k\rangle\right| \leqslant 1, \tag{11}$$

where $A_k = \hat{a}_k \cdot \vec{\sigma}$ and $B_k = \hat{b}_k \cdot \vec{\sigma}$, with $\vec{\sigma} = (\sigma_1, \sigma_2, \sigma_3)$ being the Pauli matrices and $\hat{a}_k, \hat{b}_k \in \mathbb{R}^3$ being unit and orthonormal vectors; $\langle A_k \otimes B_k\rangle = \mathrm{Tr}[\rho_{AB}(A_k \otimes B_k)]$; and $\mu = \{\hat{a}_1, \hat{a}_2, \ldots, \hat{a}_n, \hat{b}_1, \hat{b}_2, \ldots, \hat{b}_n\}$ is the set of measurement directions.

In the Hilbert-Schmidt representation, any two-qubit state can be expressed as

$$\rho_{AB} = \frac{1}{4}\left[I_2 \otimes I_2 + \vec{a} \cdot \vec{\sigma} \otimes I_2 + I_2 \otimes \vec{b} \cdot \vec{\sigma} + \sum_{i,j} t_{ij}\sigma_i \otimes \sigma_j\right], \tag{12}$$

where $\vec{a}$ and $\vec{b}$ are the local Bloch vectors, $t_{ij} = \mathrm{Tr}[\rho_{AB}(\sigma_i \otimes \sigma_j)]$, and $T_{AB} = [t_{ij}]$ is the correlation matrix. For the three measurement settings, state ρ_{AB} is F_3 steerable if and only if [52]

$$\mathcal{S}_{AB} = \mathrm{Tr}\left(T_{AB}^T T_{AB}\right) > 1, \tag{13}$$

where the superscript T represents the transpose of the correlation matrix T_{AB}. Among the three bipartite reduced states of a three-qubit state ρ_{ABC}, $\mathcal{S}_{\max}(\rho_{ABC})$ is defined as the one with the maximum steering inequality violation

$$\mathcal{S}(\rho_{ABC}) = \max\{\mathcal{S}_{AB}, \mathcal{S}_{AC}, \mathcal{S}_{BC}\}. \tag{14}$$

III. GMC VERSUS GGM

The exact relation between the GMC and GGM for three-qubit states is derived in this section.

Theorem 1. For a three-qubit pure state $|\psi\rangle$, the GGM and GMC satisfy the following relation:

$$[2\mathcal{G}(|\psi\rangle) - 1]^2 + \mathcal{C}(|\psi\rangle)^2 = 1, \tag{15}$$

where $0 \leqslant \mathcal{G}(|\psi\rangle) \leqslant 1/2$ and $0 \leqslant \mathcal{C}(|\psi\rangle) \leqslant 1$.

Proof. For a three-qubit pure state $|\psi\rangle$, the GGM is given by

$$\mathcal{G}(|\psi\rangle) = 1 - \max\{\lambda_1, \lambda_3, \lambda_5\} = \min\{\lambda_2, \lambda_4, \lambda_6\}, \tag{16}$$

where λ_1, λ_3, and λ_5 are the bigger eigenvalues of the reduced density matrices ρ_A, ρ_B, and ρ_C, respectively, and λ_2, λ_4, and λ_6 are the smaller ones. The second equation is obtained from the trace condition of the reduced density matrices,

$$\lambda_1 + \lambda_2 = 1, \quad \lambda_3 + \lambda_4 = 1, \quad \lambda_5 + \lambda_6 = 1. \tag{17}$$

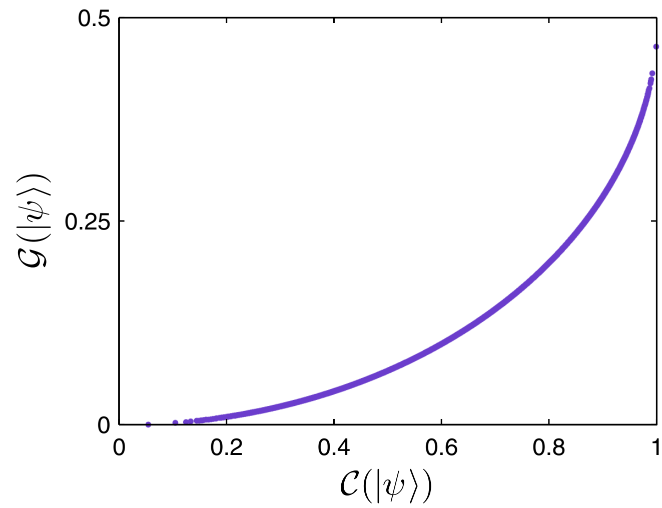

FIG. 1. Exact functional relation between the GGM $\mathcal{G}(|\psi\rangle)$ and the GMC $\mathcal{C}(|\psi\rangle)$ for 10^5 Haar randomly generated three-qubit pure states. The x and y axes are dimensionless.

If we assume that

$$\lambda_2 \leqslant \lambda_4, \quad \lambda_2 \leqslant \lambda_6, \tag{18}$$

then we can get the GGM of the state $|\psi\rangle$ as

$$\mathcal{G}(|\psi\rangle) = \lambda_2. \tag{19}$$

The GMC of three-qubit pure states is given by

$$\mathcal{C}(|\psi\rangle) = \min_i \sqrt{2\left[1 - \mathrm{Tr}\left(\rho_i^2\right)\right]}, \tag{20}$$

where $i \in \{A, B, C\}$ and $\mathrm{Tr}(\rho_i^2)$ is the purity of the reduced density matrices. It can be calculated as

$$\mathrm{Tr}\left(\rho_A^2\right) = \lambda_1^2 + \lambda_2^2, \quad \mathrm{Tr}\left(\rho_B^2\right) = \lambda_3^2 + \lambda_4^2, \quad \mathrm{Tr}\left(\rho_C^2\right) = \lambda_5^2 + \lambda_6^2. \tag{21}$$

From Eqs. (17), (18), and (21), we can show that (see Appendix A)

$$\mathrm{Tr}\left(\rho_A^2\right) \geqslant \mathrm{Tr}\left(\rho_B^2\right), \quad \mathrm{Tr}\left(\rho_A^2\right) \geqslant \mathrm{Tr}\left(\rho_C^2\right). \tag{22}$$

This gives

$$\mathcal{C}(|\psi\rangle) = \sqrt{2\left[1 - \mathrm{Tr}\left(\rho_A^2\right)\right]}. \tag{23}$$

From Eqs. (17), (19), (21), and (23), we can finally obtain the relation between the GGM and GMC as Eq. (15). The above relation also holds if we assume λ_4 or λ_6 is the smallest one among the eigenvalues λ_2, λ_4, and λ_6. ■

In Fig. 1, we plot the exact functional relation between the GGM and GMC for 10^5 Haar randomly generated three-qubit pure states [60]. The results show that the GGM is one quarter of an elliptic curve with respect to the GMC, whose center point is located at (0,0.5). The minor axis of the ellipse lies at the longitudinal axis whose value is 1, and the major axis has a value of 2.

With Theorem 1, we can prove the following corollary.

Corollary 1. For a three-qubit mixed state ρ, the relation between the GGM and GMC is

$$[2\mathcal{G}(\rho)-1]^2+\mathcal{C}(\rho)^2 \leqslant 1, \tag{24}$$

where $0 \leqslant \mathcal{G}(\rho) \leqslant 1/2$ and $0 \leqslant \mathcal{C}(\rho) \leqslant 1$.

Proof. For the three-qubit pure state, the functional relation in Eq. (15) can be rewritten as

$$\mathcal{G}(|\psi\rangle)=\frac{1}{2}(1-\sqrt{1-\mathcal{C}(|\psi\rangle)^2})=H(\mathcal{C}(|\psi\rangle)). \tag{25}$$

It can be found that the function H is monotonic within the definition domain, and it is convex with respect to $\mathcal{C}(|\psi\rangle)$. For a mixed state ρ, both $\mathcal{G}(\rho)$ and $\mathcal{C}(\rho)$ are defined by the infimum over all feasible decompositions. In fact, they share the same optimal decomposition $\sum_j p_j|\psi_j\rangle\langle\psi_j|$ because of the monotonic functional relation between them. Hence, from Eqs. (3) and (5), we have

$$\begin{aligned} H[\mathcal{C}(\rho)] &= H\left[\sum_j p_j\mathcal{C}(\psi_j)\right] \leqslant \sum_j p_j H[\mathcal{C}(\psi_j)] \\ &= \sum_j p_j\mathcal{G}(\psi_j)=\mathcal{G}(\rho). \end{aligned} \tag{26}$$

Finally, we can obtain the relation in Eq. (24). ■

IV. GENUINE TRIPARTITE ENTANGLEMENT VERSUS FIRST-ORDER COHERENCE

In this section, we present the intrinsic relations between first-order coherence and genuine tripartite entanglement including the GMC and concurrence fill for three-qubit states. These correlative relations may deepen the understanding of the interconversions among coherence and different measures of quantum correlations in the framework of QRTs.

In order to express these relations in a more explicit manner, here, we introduce three boundary states with a single parameter. The first one is the generalized Greenberger-Horne-Zeilinger (GHZ) state, which can exhibit the maximum first-order coherence value for a fixed amount of genuine tripartite entanglement, i.e.,

$$|\psi\rangle_\alpha=\cos\alpha|i,j,k\rangle+\sin\alpha|\bar{i},\bar{j},\bar{k}\rangle, \tag{27}$$

where $i,j,k\in\{0,1\}$ and the overbar means taking the opposite value. Since their performances are equivalent, we take the following states as an example in the calculation:

$$|\psi\rangle_\alpha=\cos\alpha|000\rangle+\sin\alpha|111\rangle. \tag{28}$$

The second boundary state is a single-parameter family of three-qubit pure states with

$$|\psi\rangle_m=\frac{|000\rangle+m(|010\rangle+|101\rangle)+|111\rangle}{\sqrt{2+2m^2}}, \tag{29}$$

where $m\in[0,1]$. For $m\in[0,1)$, the state belongs to the GHZ class, and the state belongs to the W class when $m=1$. Interestingly, this class of state is also regarded as the maximally steering inequality violating states [53], maximally Bell inequality violating states [61], and the maximally dense coding capable states [62].

The third one is a single-parameter family of separable three-qubit pure states which is located in the upper boundary of the relation between the maximum steering inequality violation and first-order coherence. It is given by

$$|\psi\rangle_\theta=|i\rangle(\cos\theta|j,k\rangle+\sin\theta|\bar{j},\bar{k}\rangle), \tag{30}$$

where $i,j,k\in\{0,1\}$ and $|i\rangle$ also can represent the second or third qubit. We choose the following states as an example:

$$|\psi\rangle_\theta=\cos\theta|001\rangle+\sin\theta|100\rangle. \tag{31}$$

Note that the above three boundary states always form a trilateral region in the investigation of the unification of different measures of quantum resources in which all three-qubit pure states will be included.

A. First-order coherence versus the GMC

The trade-off relation between first-order coherence and the GMC for three-qubit states is derived in this section.

Theorem 2. If a three-qubit pure state $|\psi\rangle$ has the same value of the GMC with boundary states $|\psi\rangle_\alpha$ and $|\psi\rangle_m$, the first-order coherence of these three states satisfies the ordering $\mathcal{D}(|\psi\rangle_m)\leqslant\mathcal{D}(|\psi\rangle)\leqslant\mathcal{D}(|\psi\rangle_\alpha)$. The trade-off relation of the GMC and first-order coherence is given by

$$\begin{aligned} &\mathcal{C}(|\psi\rangle)^2+\mathcal{D}(|\psi\rangle)^2\leqslant 1,\\ &\mathcal{C}(|\psi\rangle)^2+3\mathcal{D}(|\psi\rangle)^2\geqslant 1. \end{aligned} \tag{32}$$

Proof. For state $|\psi\rangle$, from Eqs. (9) and (10), the square of its first-order coherence can be obtained as

$$\mathcal{D}(|\psi\rangle)^2=\tfrac{2}{3}\big[\mathrm{Tr}(\rho_A^2)+\mathrm{Tr}(\rho_B^2)+\mathrm{Tr}(\rho_C^2)\big]-1. \tag{33}$$

Assuming that

$$\mathrm{Tr}(\rho_A^2)\geqslant\mathrm{Tr}(\rho_B^2),\quad \mathrm{Tr}(\rho_A^2)\geqslant\mathrm{Tr}(\rho_C^2), \tag{34}$$

we can obtain

$$\mathcal{C}(|\psi\rangle)^2=2\big[1-\mathrm{Tr}(\rho_A^2)\big]. \tag{35}$$

From this inequality,

$$\mathrm{Tr}(\rho_B^2)+\mathrm{Tr}(\rho_C^2)\leqslant 2\mathrm{Tr}(\rho_A^2), \tag{36}$$

we can see that (Appendix B 1)

$$2\big[1-\mathrm{Tr}(\rho_A^2)\big]+\tfrac{2}{3}\big[\mathrm{Tr}(\rho_A^2)+\mathrm{Tr}(\rho_B^2)+\mathrm{Tr}(\rho_C^2)\big]-1\leqslant 1. \tag{37}$$

Therefore, for state $|\psi\rangle$, substituting Eqs. (33) and (35) into Eq. (37), we get the upper boundary of the relation between the GMC and first-order coherence,

$$\mathcal{C}(|\psi\rangle)^2+\mathcal{D}(|\psi\rangle)^2\leqslant 1. \tag{38}$$

Based on the fact that $\mathrm{Tr}(\rho_i^2)\geqslant\frac{1}{2}$, where $i\in\{A,B,C\}$, we have

$$\mathrm{Tr}(\rho_B^2)+\mathrm{Tr}(\rho_C^2)\geqslant 1. \tag{39}$$

By this inequality, we can prove that (Appendix B 2)

$$2\big[1-\mathrm{Tr}(\rho_A^2)\big]+2\big[\mathrm{Tr}(\rho_A^2)+\mathrm{Tr}(\rho_B^2)+\mathrm{Tr}(\rho_C^2)\big]-3\geqslant 1. \tag{40}$$

Similarly, we obtain the lower boundary of the relation between the GMC and first-order coherence as

$$\mathcal{C}(|\psi\rangle)^2+3\mathcal{D}(|\psi\rangle)^2\geqslant 1. \tag{41}$$

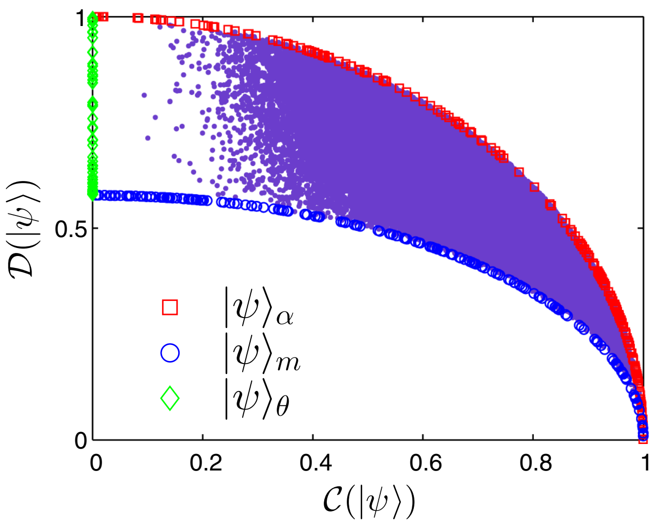

FIG. 2. Trade-off relation between the first-order coherence $\mathcal{D}(|\psi\rangle)$ and the GMC $\mathcal{C}(|\psi\rangle)$ for 10^5 Haar randomly generated three-qubit pure states. The red squares lie at the upper boundary with state $|\psi\rangle_\alpha$; state $|\psi\rangle_m$, denoted by blue circles, is located at the lower boundary, and the green diamonds represent state $|\psi\rangle_\theta$, which lies at the y axis. The x and y axes are dimensionless.

Moreover, the relations are also valid if we assume $\mathrm{Tr}(\rho_B^2)$ or $\mathrm{Tr}(\rho_C^2)$ is the largest one among the three purities of subsystems ρ_A, ρ_B, and ρ_C.

The GMC and first-order coherence of states $|\psi\rangle_\alpha$ and $|\psi\rangle_m$, from Eqs. (10) and (20), are given by

$$\mathcal{C}(|\psi\rangle_\alpha) = \sqrt{2(1-\cos^4\alpha - \sin^4\alpha)}, \tag{42}$$

$$\mathcal{D}(|\psi\rangle_\alpha) = |\cos 2\alpha|, \tag{43}$$

$$\mathcal{C}(|\psi\rangle_m) = \frac{1-m^2}{1+m^2}, \tag{44}$$

$$\mathcal{D}(|\psi\rangle_m) = \frac{2m}{\sqrt{3}(1+m^2)}, \tag{45}$$

respectively. We can find that

$$\mathcal{C}(|\psi\rangle_\alpha)^2 + \mathcal{D}(|\psi\rangle_\alpha)^2 = 1, \tag{46}$$

$$\mathcal{C}(|\psi\rangle_m)^2 + 3\mathcal{D}(|\psi\rangle_m)^2 = 1, \tag{47}$$

which imply that states $|\psi\rangle_\alpha$ and $|\psi\rangle_m$ are the upper and lower boundary states. ■

In Fig. 2, we plot how the first-order coherence changes with respect to the GMC for 10^5 Haar randomly generated three-qubit pure states. The red squares donating state $|\psi\rangle_\alpha$ are located at the upper boundary, which satisfies the relation between first-order coherence and the GMC in Eq. (46). The blue circles at the lower boundary indicate that the two quantum resources of state $|\psi\rangle_m$ fulfill the relation in Eq. (47). The 10^5 Haar randomly generated three-qubit pure states are included in the trilateral region formed by states $|\psi\rangle_\alpha$, $|\psi\rangle_m$, and $|\psi\rangle_\theta$, meaning their first-order coherence and GMC obey the inequalities in Eq. (32). Moreover, we find the first-order coherence increases (decreases) with the decrease (increase) of the GMC, showing a trade-off. rgb]0.00,0,0 The trade-off relation can be generalized to mixed states by the convexity properties of the first-order coherence and GMC.

Corollary 2. For an arbitrary three-qubit mixed state ρ, the trade-off relation of the GMC and first-order coherence is as follows:

$$\mathcal{C}(\rho)^2 + \mathcal{D}(\rho)^2 \leqslant 1. \tag{48}$$

The upper boundary states are still states $|\psi\rangle_\alpha$.

Proof. For subsystem ρ_A of a three-qubit mixed state ρ_{ABC}, the first-order coherence is given by

$$\begin{aligned}\mathcal{D}(\rho_A) &= \sqrt{2\,\mathrm{Tr}\left(\rho_A^2\right) - 1}\\ &= \sqrt{2\left(\lambda_1^2+\lambda_2^2\right)-1}\\ &= |2\lambda_1 - 1|,\end{aligned} \tag{49}$$

which is a convex function. Similarly, $\mathcal{D}(\rho_B)$ and $\mathcal{D}(\rho_C)$ are also convex functions. The first-order coherence of state ρ_{ABC}, as the vector composition of $\mathcal{D}(\rho_i)$ and $h(x_1,x_2,x_3) = [(x_1^2+x_2^2+x_3^2)/3]^{1/2}$, is also a convex function [63]. In addition, Eq. (38) can be rewritten as

$$\mathcal{D}(|\psi\rangle) \leqslant \sqrt{1-\mathcal{C}(|\psi\rangle)^2}. \tag{50}$$

Let $U[\mathcal{C}(|\psi\rangle)] = \sqrt{1-\mathcal{C}(|\psi\rangle)^2}$; then it can be found that U is a concave and monotonically decreasing function with respect to $\mathcal{C}(|\psi\rangle)$. Then, we get

$$\begin{aligned}\mathcal{D}(\rho) &\leqslant \sum_i p_i \mathcal{D}(\psi_i) \leqslant \sum_i p_i\sqrt{1-\mathcal{C}(\psi_i)^2}\\ &\leqslant \sqrt{1-\left[\sum_i p_i\mathcal{C}(\psi_i)\right]^2}\\ &\leqslant \sqrt{1-\mathcal{C}(\rho)^2},\end{aligned} \tag{51}$$

i.e.,

$$\mathcal{C}(\rho)^2 + \mathcal{D}(\rho)^2 \leqslant 1. \tag{52}$$

■

To summarize, if the two measures of quantum resources satisfy the following three conditions, the trade-off relation between the two quantum resources for pure states can be generalized to the case in mixed states: (i) the two measures are convex functions; (ii) the value of one measure is less than or equal to the function ξ, which depends on another measure; and (iii) ξ is a concave and monotonically decreasing function.

B. First-order coherence versus concurrence fill

The trade-off relation between first-order coherence and concurrence fill for three-qubit pure states is derived in this section.

Theorem 3. If a three-qubit pure state $|\psi\rangle$ has the same value of concurrence fill with states $|\psi\rangle_\alpha$ and $|\psi\rangle_m$, the first-order coherence of these three states satisfies the ordering $\mathcal{D}(|\psi\rangle_m) \leqslant \mathcal{D}(|\psi\rangle) \leqslant \mathcal{D}(|\psi\rangle_\alpha)$. The trade-off relation of the concurrence fill and first-order coherence is given by

$$\mathcal{F}(|\psi\rangle)+\mathcal{D}(|\psi\rangle)^2 \leqslant 1,$$
$$\mathcal{F}(|\psi\rangle)^4+[3\mathcal{D}(|\psi\rangle)^2 1]^2[3\mathcal{D}(|\psi\rangle)^4-2\mathcal{D}(|\psi\rangle)^2-1]\geqslant 0, \tag{53}$$

where $0 \leqslant \mathcal{D}(|\psi\rangle) \leqslant 1/\sqrt{3}$ for the second inequality. rgb]0.00,0,0The first inequality is also valid for the three-qubit mixed states.

Proof. For state $|\psi\rangle$, substituting Eq. (21) into Eq. (33), its first-order coherence can be written as

$$\mathcal{D}(|\psi\rangle)^2=\tfrac{2}{3}\left(\lambda_1^2+\lambda_2^2+\lambda_3^2+\lambda_4^2+\lambda_5^2+\lambda_6^2\right)-1. \tag{54}$$

From Eqs. (7) and (8), we can get

$$Q=2(\lambda_1\lambda_2+\lambda_3\lambda_4+\lambda_5\lambda_6). \tag{55}$$

Then we can obtain the relation between $\mathcal{D}(|\psi\rangle)$ and Q:

$$\mathcal{D}(|\psi\rangle)^2=1-\tfrac{2}{3}Q. \tag{56}$$

For simplicity, we define $C^2_{A(BC)}, C^2_{B(AC)}$, and $C^2_{C(AB)}$ as a, b, and c, respectively. By the mean-value inequality, we have

$$(Q-a)(Q-b)(Q-c)\leqslant\left(\frac{Q}{3}\right)^3. \tag{57}$$

Note that the summation of three terms on each side of the inequality is equal to Q. As a result, we find that (Appendix C 1)

$$\left[\tfrac{16}{3}Q(Q-a)(Q-b)(Q-c)\right]^{1/4}+1-\tfrac{2}{3}Q\leqslant 1. \tag{58}$$

Substituting Eqs. (6) and (56) into Eq. (58), we have

$$\mathcal{F}(|\psi\rangle)+\mathcal{D}(|\psi\rangle)^2\leqslant 1. \tag{59}$$

On the other hand, from Eq. (56) and the relation $0\leqslant\mathcal{D}(|\psi\rangle)\leqslant 1/\sqrt{3}$, we can obtain $1\leqslant Q\leqslant 3/2$. Since $0\leqslant a,b,c\leqslant 1$, we get $Q-1\leqslant Q-a, Q-b, Q-c\leqslant 2-Q$. Thus, using the mean-value inequality, we have

$$(2-Q)(Q-1)^2\leqslant(Q-a)(Q-b)(Q-c). \tag{60}$$

Consequently, we can see that (Appendix C 2)

$$\tfrac{16}{3}Q(Q-a)(Q-b)(Q-c)+\left[3\left(1-\tfrac{2}{3}Q\right)-1\right]^2$$
$$\times\left[3\left(1-\tfrac{2}{3}Q\right)^2-2\left(1-\tfrac{2}{3}Q\right)-1\right]\geqslant 0. \tag{61}$$

In a similar way, we have

$$\mathcal{F}(|\psi\rangle)^4+[3\mathcal{D}(|\psi\rangle)^2-1]^2[3\mathcal{D}(|\psi\rangle)^4-2\mathcal{D}(|\psi\rangle]^2-1)\geqslant 0. \tag{62}$$

The concurrence fills of states $|\psi\rangle_\alpha$ and $|\psi\rangle_m$, from Eq. (6), are given by

$$\mathcal{F}(|\psi\rangle_\alpha)=\sin^2(2\alpha), \tag{63}$$

$$\mathcal{F}(|\psi\rangle_m)=\frac{(1-m^2)[(1+6m^2+m^4)(3+2m^2+3m^4)]^{1/4}}{3^{1/4}(1+m^2)^2}. \tag{64}$$

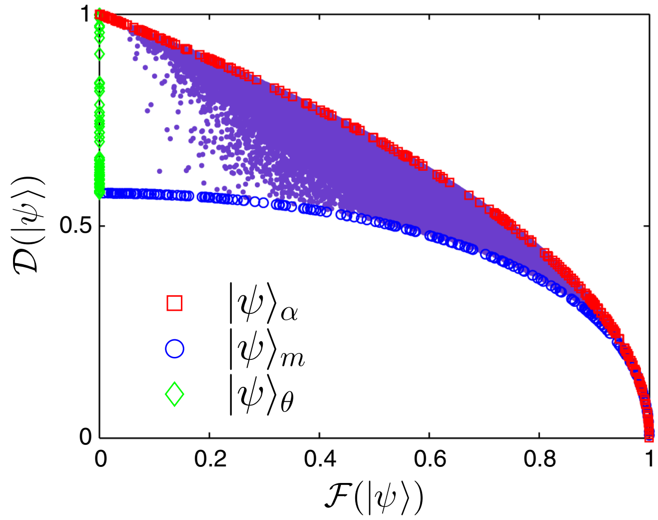

FIG. 3. Trade-off relation between the first-order coherence $\mathcal{D}(|\psi\rangle)$ and the concurrence fill $\mathcal{F}(|\psi\rangle)$ for 10^5 Haar randomly generated three-qubit pure states. The red squares lie at the upper boundary with state $|\psi\rangle_\alpha$; state $|\psi\rangle_m$, denoted by blue circles, is located at the lower boundary, and the green diamonds represent state $|\psi\rangle_\theta$, which lies at the y axis. The x and y axes are dimensionless.

Together with Eqs. (43) and (45), we can obtain the following relations:

$$\mathcal{F}(|\psi\rangle_\alpha)+\mathcal{D}(|\psi\rangle_\alpha)^2=1, \tag{65}$$

$$\mathcal{F}(|\psi\rangle_m)^4+(3\mathcal{D}(|\psi\rangle_m)^2-1)^2$$
$$\times[3\mathcal{D}(|\psi\rangle_m)^4-2\mathcal{D}(|\psi\rangle_m)^2-1]=0, \tag{66}$$

which imply that states $|\psi\rangle_\alpha$ and $|\psi\rangle_m$ are the upper and lower boundary states, respectively.

The functional relation in Eq. (59) can be rewritten as

$$\mathcal{D}(|\psi\rangle)\leqslant\sqrt{1-\mathcal{F}(|\psi\rangle)}; \tag{67}$$

the right side of the inequality is a concave and monotonically decreasing function. On the other hand, concurrence fill is a convex function under mixing [17]. Like in Eq. (51), we can obtain

$$\mathcal{F}(\rho)+\mathcal{D}(\rho)^2\leqslant 1, \tag{68}$$

where ρ is an arbitrary three-qubit mixed state. ■

Figure 3 plots the relation between the first-order coherence and the concurrence fill for 10^5 Haar randomly generated three-qubit pure states. We can see that states $|\psi\rangle_\alpha$ (red squares) and $|\psi\rangle_m$ (blue circles) are located at the upper and lower boundaries, respectively, which means that their first-order coherences and concurrence fills satisfy the relations in Eqs. (65) and (66), respectively. Together with state $|\psi\rangle_\theta$ on the y axis, they form a trilateral region, which includes all three-qubit pure states. Also, Fig. 3 shows that a trade-off relation exists between the first-order coherence and concurrence fill for arbitrary three-qubit pure states.

V. THE MAXIMUM STEERING INEQUALITY VIOLATION VERSUS CONCURRENCE FILL

Quantum steering describes an important trait of the quantum world in which one system can immediately affect another one by local measurements. The concurrence fill was introduced as a good triangle measure of tripartite entanglement in 2021 and can detect genuine three-qubit entanglement faithfully [17]. Here, our aim is to study the relation between the maximum steering inequality violation and concurrence fill.

Theorem 4. If an arbitrary three-qubit state ρ has the same value of concurrence fill as state $|\psi\rangle_m$, the maximum steering inequality violation of these two states satisfies the ordering $\mathcal{S}(\rho) \leqslant \mathcal{S}(|\psi\rangle_m)$. The trade-off relation of the maximum steering inequality violation and concurrence fill is given by

$$48\mathcal{F}(\rho)^4 + [\mathcal{S}(\rho) - 3]^2[\mathcal{S}(\rho) + 1][\mathcal{S}(\rho) - 7] \leqslant 0. \quad (69)$$

Proof. Any three-qubit state ρ_{ABC} can be written as

$$\begin{aligned}\rho_{ABC} = \frac{1}{8}\Bigg[&\mathbb{I}\otimes\mathbb{I}\otimes\mathbb{I} + \vec{A}\cdot\vec{\sigma}\otimes\mathbb{I}\otimes\mathbb{I} + \mathbb{I}\otimes\vec{B}\cdot\vec{\sigma}\otimes\mathbb{I}\\ &+\mathbb{I}\otimes\mathbb{I}\otimes\vec{C}\cdot\vec{\sigma} + \sum_{ij} t_{ij}^{AB}\sigma_i\otimes\sigma_j\otimes\mathbb{I}\\ &+\sum_{ik} t_{ik}^{AC}\sigma_i\otimes\mathbb{I}\otimes\sigma_k + \sum_{jk} t_{jk}^{BC}\mathbb{I}\otimes\sigma_j\otimes\sigma_k\\ &+\sum_{ijk} t_{ijk}^{ABC}\sigma_i\otimes\sigma_j\otimes\sigma_k\Bigg].\end{aligned} \quad (70)$$

This gives

$$\mathrm{Tr}\left(\rho_A^2\right) = \frac{1+\vec{A}^2}{2}, \quad \mathrm{Tr}\left(\rho_{BC}^2\right) = \frac{1}{4}(1+\vec{B}^2+\vec{C}^2+\mathcal{S}_{BC}). \quad (71)$$

Similarly, we have

$$\begin{aligned}\mathrm{Tr}\left(\rho_B^2\right) &= \frac{1+\vec{B}^2}{2}, \quad \mathrm{Tr}\left(\rho_{AC}^2\right) = \frac{1}{4}(1+\vec{A}^2+\vec{C}^2+\mathcal{S}_{AC}),\\ \mathrm{Tr}\left(\rho_C^2\right) &= \frac{1+\vec{C}^2}{2}, \quad \mathrm{Tr}\left(\rho_{AB}^2\right) = \frac{1}{4}(1+\vec{A}^2+\vec{B}^2+\mathcal{S}_{AB}).\end{aligned} \quad (72)$$

If ρ_{ABC} is a pure state, by the Schmidt decomposition, we have $\mathrm{Tr}(\rho_i^2) = \mathrm{Tr}(\rho_{jk}^2)$ for $i \neq j \neq k,\ i, j, k \in \{A, B, C\}$. From Eqs. (71) and (72), we can write $\mathcal{S}_{AB}$ as a function of the purities of the subsystems,

$$\mathcal{S}_{AB} = 4\mathrm{Tr}\left(\rho_C^2\right) - 2\mathrm{Tr}\left(\rho_A^2\right) - 2\mathrm{Tr}\left(\rho_B^2\right) + 1. \quad (73)$$

Combining the above equation and Eqs. (8), (17), and (21), we can obtain (Appendix D 1)

$$\mathcal{S}_{AB} = a + b - 2c + 1. \quad (74)$$

Similarly, we get

$$\begin{aligned}\mathcal{S}_{AC} &= a + c - 2b + 1,\\ \mathcal{S}_{BC} &= b + c - 2a + 1.\end{aligned} \quad (75)$$

Assume that the bipartite steering of the subsystem S_{AB} is the largest one among S_{AB}, S_{AC}, and S_{BC}, i.e., $S_{AB} \geqslant S_{AC}$, $S_{AB} \geqslant S_{BC}$, Thus, we get the maximum steering inequality violation

$$\mathcal{S}(|\psi\rangle) = \mathcal{S}_{AB}. \quad (76)$$

From Eqs. (74) and (75), we have $a \geqslant c$, $b \geqslant c$, and $0 \leqslant a + b - 2c \leqslant 2$. By these constraints, we can show that (Appendix D 2)

$$4(Q-a) + 4(Q-b) \leqslant 2[2 - (a+b-2c)]. \quad (77)$$

Using the mean-value inequality, we get

$$4(Q-a)4(Q-b) \leqslant [2-(a+b-2c)]^2. \quad (78)$$

Like in Eq. (77), we can obtain

$$\begin{aligned}4(Q-c) &\leqslant 2 + a + b - 2c,\\ 4Q &\leqslant 6 - (a+b-2c).\end{aligned} \quad (79)$$

As a consequence, we have

$$\begin{aligned}4(Q-a)4(Q-b)4(Q-c)4Q &\leqslant [2-(a+b-2c)]^2\\ &\times (2+a+b-2c)[6-(a+b-2c)].\end{aligned} \quad (80)$$

From this inequality, we can see that (Appendix D 3)

$$\begin{aligned}&48\times\tfrac{16}{3}Q(Q-a)(Q-b)(Q-c) + (a+b-2c+1-3)^2\\ &(a+b-2c+1+1)(a+b-2c+1-7) \leqslant 0.\end{aligned} \quad (81)$$

Finally, substituting Eqs. (6) and (79) into Eq. (81), we obtain the trade-off relation of the maximum steering inequality violation and concurrence fill for three-qubit pure states as

$$48\mathcal{F}(|\psi\rangle)^4 + [\mathcal{S}(|\psi\rangle) - 3]^2[\mathcal{S}(|\psi\rangle) + 1][\mathcal{S}(|\psi\rangle) - 7] \leqslant 0. \quad (82)$$

The trade-off relation also holds for the situations in which the bipartite steering $\mathcal{S}_{AC}$ or $\mathcal{S}_{BC}$ is the largest one among $\mathcal{S}_{AB}$, $\mathcal{S}_{AC}$, and $\mathcal{S}_{BC}$. Equation (82) can be denoted by an equivalent form with

$$\mathcal{F}(|\psi\rangle) \leqslant \left[-\tfrac{1}{48}[\mathcal{S}(|\psi\rangle) - 3]^2[\mathcal{S}(|\psi\rangle) + 1][\mathcal{S}(|\psi\rangle) - 7]\right]^{1/4}, \quad (83)$$

whose right side is still a concave and monotonically decreasing function with respect to $\mathcal{S}(|\psi\rangle)$.

If ρ_{ABC} is a mixed state, the maximum steering inequality violation is also a convex function [52]. By a derivation similar to Eq. (51), we find that Eq. (69) holds for the three-qubit mixed state.

The maximum steering inequality violation of state $|\psi\rangle_m$, from Eq. (14), can be calculated as

$$\mathcal{S}(|\psi\rangle_m) = \frac{1+10m^2+m^4}{(1+m^2)^2}. \quad (84)$$

Together with Eq. (64), we can obtain

$$48\mathcal{F}(|\psi\rangle_m)^4 + [\mathcal{S}(|\psi\rangle_m) - 3]^2[\mathcal{S}(|\psi\rangle_m) + 1][\mathcal{S}(|\psi\rangle_m) - 7] = 0, \quad (85)$$

which implies that state $|\psi\rangle_m$ is the upper boundary states. ■

In Fig. 4, we plot the relation between the maximum steering inequality violation and the concurrence fill for 10^5 Haar randomly generated three-qubit pure states. We can see that the state $|\psi\rangle_m$ is located at the upper boundary (blue circles),

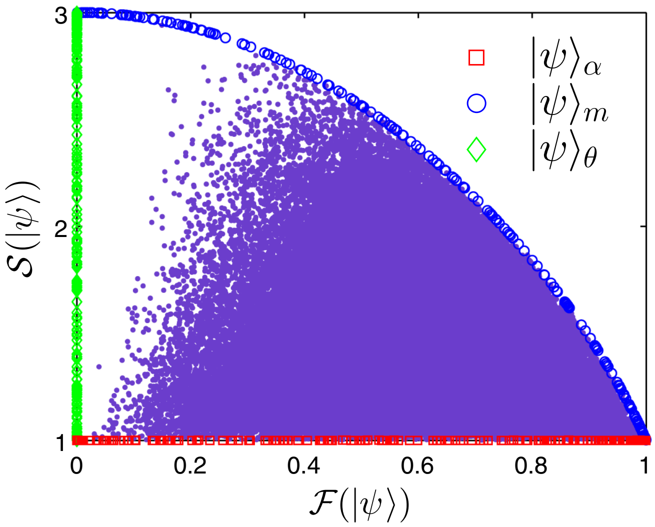

FIG. 4. Trade-off relation between the maximum steering inequality violation $\mathcal{S}(|\psi\rangle)$ and the concurrence fill $\mathcal{F}(|\psi\rangle)$ for 10^5 Haar randomly generated three-qubit pure states. The blue circles at the upper boundary represent sate $|\psi\rangle_m$, and states $|\psi\rangle_\alpha$ and $|\psi\rangle_\theta$ are located at the x and y axes, respectively. The x and y axes are dimensionless.

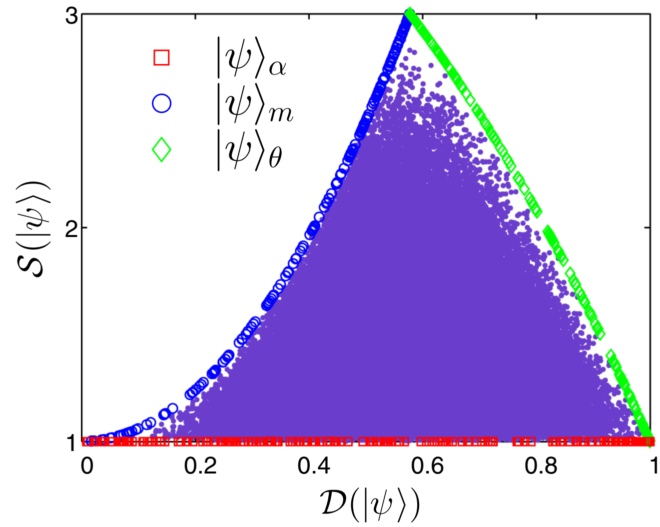

FIG. 5. The close relation between the maximum steering inequality violation $\mathcal{S}(|\psi\rangle)$ and the first-order coherence $\mathcal{D}(|\psi\rangle)$ for 10^5 Haar randomly generated three-qubit pure states. States $|\psi\rangle_m$ and $|\psi\rangle_\theta$ are located at the left and right upper boundaries, respectively, and state $|\psi\rangle_\alpha$ is on the x axis. The x and y axes are dimensionless.

suggesting that its maximum steering inequality violation and concurrence fill satisfy Eq. (85). In particular, states $|\psi\rangle_\alpha$ and $|\psi\rangle_\theta$ are on the x and y axes, respectively.

VI. THE MAXIMUM STEERING INEQUALITY VIOLATION VERSUS FIRST-ORDER COHERENCE

The close relation between the maximum steering inequality violation and first-order coherence for three-qubit pure states is derived in this section.

Theorem 5. If a three-qubit pure state $|\psi\rangle$ has the same value of first-order coherence as state $|\psi\rangle_m$ or $|\psi\rangle_\theta$, the maximum steering inequality violation of these three states satisfies the ordering $\mathcal{S}(|\psi\rangle) \leqslant \mathcal{S}(|\psi\rangle_m)$ or $\mathcal{S}(|\psi\rangle) \leqslant \mathcal{S}(|\psi\rangle_\theta)$. The relation between the maximum steering inequality violation and first-order coherence is given by

$$\mathcal{S}(|\psi\rangle) - 6\mathcal{D}(|\psi\rangle)^2 \leqslant 1, \quad 0 \leqslant \mathcal{D}(|\psi\rangle) < \frac{1}{\sqrt{3}},$$
$$\mathcal{S}(|\psi\rangle) + 3\mathcal{D}(|\psi\rangle)^2 \leqslant 4, \quad \frac{1}{\sqrt{3}} \leqslant \mathcal{D}(|\psi\rangle) \leqslant 1. \tag{86}$$

Proof. For a three-qubit pure state $|\psi\rangle$, we assume that $\mathcal{S}(|\psi\rangle) = \mathcal{S}_{AB}$. Like in Eq. (39), we have

$$\mathrm{Tr}(\rho_A^2) + \mathrm{Tr}(\rho_B^2) \geqslant 1. \tag{87}$$

By this inequality, one can show that (see Appendix E 1)

$$4\mathrm{Tr}(\rho_C^2) - 2\mathrm{Tr}(\rho_A^2) - 2\mathrm{Tr}(\rho_B^2) + 1 - 6\left\{\tfrac{2}{3}\left[\mathrm{Tr}(\rho_A^2) + \mathrm{Tr}(\rho_B^2) + \mathrm{Tr}(\rho_C^2)\right] - 1\right\} \leqslant 1. \tag{88}$$

From Eqs. (33) and (73), we can obtain

$$\mathcal{S}(|\psi\rangle) - 6\mathcal{D}(|\psi\rangle)^2 \leqslant 1. \tag{89}$$

On the other hand, from the inequality $\mathrm{Tr}(\rho_C^2) \leqslant 1$, we can find that (Appendix E 2)

$$4\mathrm{Tr}(\rho_C^2) - 2\mathrm{Tr}(\rho_A^2) - 2\mathrm{Tr}(\rho_B^2) + 1 + 3\left\{\tfrac{2}{3}\left[\mathrm{Tr}(\rho_A^2) + \mathrm{Tr}(\rho_B^2) + \mathrm{Tr}(\rho_C^2)\right] - 1\right\} \leqslant 4; \tag{90}$$

then we have

$$\mathcal{S}(|\psi\rangle) + 3\mathcal{D}(|\psi\rangle)^2 \leqslant 4. \tag{91}$$

The close relation in Eq. (86) holds when $\mathcal{S}(|\psi\rangle) = \mathcal{S}_{AC}$ or $\mathcal{S}(|\psi\rangle) = \mathcal{S}_{BC}$.

The maximum steering inequality violation and first-order coherence of the state $|\psi\rangle_\theta$, from Eqs. (10) and (14), are

$$\mathcal{S}(|\psi\rangle_\theta) = 2 - \cos(4\theta), \tag{92}$$

$$\mathcal{D}(|\psi\rangle_\theta) = \sqrt{\frac{2 + \cos(4\theta)}{3}}. \tag{93}$$

Together with Eqs. (45) and (84), we can obtain

$$\mathcal{S}(|\psi\rangle_m) - 6\mathcal{D}(|\psi\rangle_m)^2 = 1, \tag{94}$$

$$\mathcal{S}(|\psi\rangle_\theta) + 3\mathcal{D}(|\psi\rangle_\theta)^2 = 4, \tag{95}$$

which imply that states $|\psi\rangle_m$ are the upper boundary states for $0 \leqslant \mathcal{D}(|\psi\rangle) < 1/\sqrt{3}$ and states $|\psi\rangle_\theta$ are the upper boundary states for $1/\sqrt{3} \leqslant \mathcal{D}(|\psi\rangle) \leqslant 1$. ■

Figure 5 plots the relation between the maximum steering inequality violation and the first-order coherence for 10^5 Haar randomly generated three-qubit pure states. The maximum steering inequality violation increases at first and then

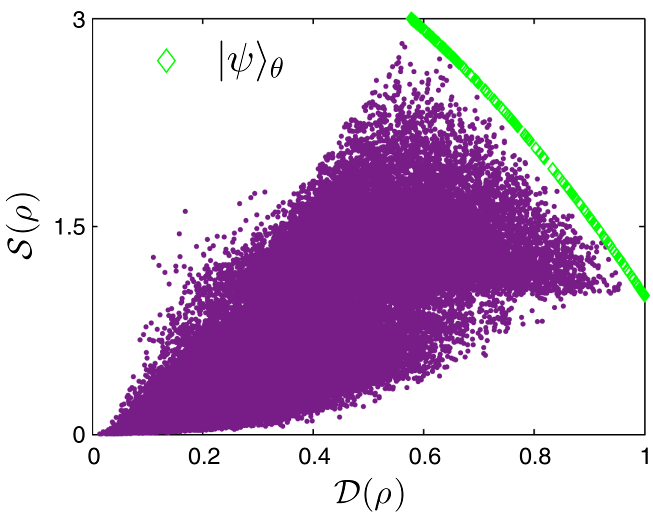

FIG. 6. The close relation between the maximum steering inequality violation $\mathcal{S}(\rho)$ and the first-order coherence $\mathcal{D}(\rho)$ for 10^5 Haar randomly generated three-qubit mixed states. The state $|\psi\rangle_\theta$ is located at the upper right boundary. The x and y axes are dimensionless.

decreases with the increase of first-order coherence. The maximum steering inequality violation approaches its maximum of 3 when the first-order coherence gets close to the critical value $1/\sqrt{3}$. States $|\psi\rangle_m$ and $|\psi\rangle_\theta$ are located at the upper left and right boundaries, respectively. The 10^5 Haar randomly generated three-qubit pure states are contained in the trilateral region.

Corollary 3. For the three-qubit mixed state ρ, the trade-off relation between the maximum steering inequality violation and first-order coherence is

$$\mathcal{S}(\rho) + 3\mathcal{D}(\rho)^2 \leqslant 4, \tag{96}$$

with $1/\sqrt{3} \leqslant \mathcal{D}(\rho) \leqslant 1$.

We plot the relation between the maximum steering inequality violation and the first-order coherence for 10^5 Haar randomly generated three-qubit mixed states in Fig. 6. We can see that state $|\psi\rangle_\theta$ is located in the upper right boundary (green diamonds), which is the same as in Fig. 5. For $1/\sqrt{3} \leqslant \mathcal{D}(\rho) \leqslant 1$, the bound shows that there is a trade-off relation between the maximum steering inequality violation and the first-order coherence for the three-qubit mixed states.

VII. SUMMARY

In summary, we proposed a general framework for unifying coherence and different measures of quantum correlations, including genuine tripartite entanglement and quantum steering, for arbitrary tripartite entanglement states. First of all, a one-to-one mapping (equality) exists between the GGM and GMC for three-qubit pure states. Subsequently, the trade-off relations between first-order coherence and genuine tripartite entanglement were established for the three-qubit states, where the genuine tripartite entanglement is quantified by the GGM, GMC, and concurrence fill. For the pure states, the results showed that the first-order coherence is constrained to a range formed by two inequalities for a fixed amount of genuine tripartite entanglement. The upper boundary states of the trade-off relation are state $|\psi\rangle_\alpha$, which possesses the maximum first-order coherence value, and $|\psi\rangle_m$ is the lower boundary state. However, only the upper boundary and the corresponding inequality are still valid for mixed states. Moreover, we investigate the trade-off relation between the maximum steering inequality violation and concurrence fill. Differently, in this case, the $|\psi\rangle_m$ state takes the maximum steering inequality violation for a given concurrence fill. In addition, we presented the close relation between the maximum steering inequality violation and first-order coherence. For pure states, it was found that the upper boundary of the maximum steering inequality violation increases at first and then decreases with the increase of first-order coherence. When a critical value of $1/\sqrt{3}$ of the first-order coherence is reached, the corresponding maximum steering inequality violation is its maximum, 3. The upper left boundary state is state $|\psi\rangle_m$, and the upper right state is another boundary state, $|\psi\rangle_\theta$. Both of them have the maximum steering inequality violation for a fixed value of first-order coherence. But only the upper right boundary and corresponding inequality can be generalized to mixed states. For these relations, the bounds allow us to quantify the maximum (minimum) value of one for a given value of the other. Studying the distribution and transformation of coherence and quantum correlations in QRTs is of great significance.

ACKNOWLEDGMENTS

This work was supported by the National Science Foundation of China (Grants No. 12004006, No. 12075001, and No. 12175001), Anhui Provincial Key Research and Development Plan (Grant No. 2022b13020004), and Anhui Provincial Natural Science Foundation (Grant No. 2008085QA43).

APPENDIX A: SUPPLEMENTARY PROOF OF GMC VERSUS GGM

Here, we give the proof of Eq. (22). From the Eqs. (17) and (21), we can obtain

$$\mathrm{Tr}(\rho_A^2) = \lambda_1^2 + \lambda_2^2 = 2\lambda_2^2 - 2\lambda_2 + 1. \tag{A1}$$

Similarly, we get

$$\mathrm{Tr}(\rho_B^2) = 2\lambda_4^2 - 2\lambda_4 + 1, \quad \mathrm{Tr}(\rho_C^2) = 2\lambda_6^2 - 2\lambda_6 + 1. \tag{A2}$$

Note that the right-hand sides of these equations take the same form as the function with $2\lambda^2 - 2\lambda + 1$, which decreases monotonically in the interval where $\lambda \in [0, 0.5]$. Since λ_2, λ_4, and λ_6 are the smaller eigenvalues of the reduced density matrices ρ_A, ρ_B, and ρ_C, respectively, we have $0 \leqslant \lambda_2, \lambda_4, \lambda_6 \leqslant 0.5$. Assuming that $\lambda_2 \leqslant \lambda_4$ and $\lambda_2 \leqslant \lambda_6$, we get

$$\mathrm{Tr}(\rho_A^2) \geqslant \mathrm{Tr}(\rho_B^2), \quad \mathrm{Tr}(\rho_A^2) \geqslant \mathrm{Tr}(\rho_C^2). \tag{A3}$$

In addition, we can obtain

$$\tfrac{1}{2} \leqslant \mathrm{Tr}(\rho_i^2) \leqslant 1, \tag{A4}$$

where $i \in \{A, B, C\}$.

APPENDIX B: SUPPLEMENTARY PROOF OF FIRST-ORDER COHERENCE VERSUS GMC

1. Proof of Equation (37)

To begin with, considering the inequality

$$\mathrm{Tr}(\rho_B^2) + \mathrm{Tr}(\rho_C^2) \leqslant 2\mathrm{Tr}(\rho_A^2), \tag{B1}$$

we have

$$-\tfrac{4}{3}\mathrm{Tr}(\rho_A^2) + \tfrac{2}{3}\mathrm{Tr}(\rho_B^2) + \tfrac{2}{3}\mathrm{Tr}(\rho_C^2) \leqslant 0. \tag{B2}$$

Then, we can obtain

$$1 - 2\mathrm{Tr}(\rho_A^2) + \tfrac{2}{3}\mathrm{Tr}(\rho_A^2) + \tfrac{2}{3}\mathrm{Tr}(\rho_B^2) + \tfrac{2}{3}\mathrm{Tr}(\rho_C^2) \leqslant 1. \tag{B3}$$

Finally, we get

$$2[1-\mathrm{Tr}(\rho_A^2)]+\tfrac{2}{3}[\mathrm{Tr}(\rho_A^2)+\mathrm{Tr}(\rho_B^2)+\mathrm{Tr}(\rho_C^2)]-1 \leqslant 1. \tag{B4}$$

2. Proof of Equation (40)

To begin with, from the inequality

$$\mathrm{Tr}(\rho_B^2) + \mathrm{Tr}(\rho_C^2) \geqslant 1, \tag{B5}$$

we have

$$-2\mathrm{Tr}(\rho_A^2)+2\mathrm{Tr}(\rho_A^2)+2\mathrm{Tr}(\rho_B^2) + 2\mathrm{Tr}(\rho_C^2) \geqslant 2. \tag{B6}$$

Then, we can see that

$$2 - 2\mathrm{Tr}(\rho_A^2)+2\mathrm{Tr}(\rho_A^2)+2\mathrm{Tr}(\rho_B^2) + 2\mathrm{Tr}(\rho_C^2) - 3 \geqslant 1. \tag{B7}$$

Finally, we get

$$2[1-\mathrm{Tr}(\rho_A^2)]+2[\mathrm{Tr}(\rho_A^2)+\mathrm{Tr}(\rho_B^2)+\mathrm{Tr}(\rho_C^2)]-3 \geqslant 1. \tag{B8}$$

APPENDIX C: SUPPLEMENTARY PROOF OF FIRST-ORDER COHERENCE VERSUS CONCURRENCE FILL

1. Proof of Equation (58)

Based on the inequality

$$(Q-a)(Q-b)(Q-c) \leqslant \left(\frac{Q}{3}\right)^3, \tag{C1}$$

we have

$$\frac{16}{3}Q(Q-a)(Q-b)(Q-c) \leqslant 16\left(\frac{Q}{3}\right)^4. \tag{C2}$$

Then, we get

$$\left[\tfrac{16}{3}Q(Q-a)(Q-b)(Q-c)\right]^{1/4} \leqslant \tfrac{2}{3}Q. \tag{C3}$$

Finally, we obtain

$$\left[\tfrac{16}{3}Q(Q-a)(Q-b)(Q-c)\right]^{1/4} + 1 - \tfrac{2}{3}Q \leqslant 1. \tag{C4}$$

2. Proof of Equation (61)

Using the inequality

$$(2-Q)(Q-1)^2 \leqslant (Q-a)(Q-b)(Q-c), \tag{C5}$$

we have

$$\begin{aligned}
\tfrac{16}{3}Q(Q-a)(Q-b)(Q-c) &\geqslant \tfrac{16}{3}(Q-1)^2(2-Q)Q \\
&= -\tfrac{1}{3}(2Q-2)^2 4(Q-2)Q \\
&= -\tfrac{1}{3}(2-2Q)^2(4Q^2-8Q) \\
&= -\tfrac{1}{3}(3-2Q-1)^2(4Q^2-12Q+9+4Q-9) \\
&= -\tfrac{1}{3}\left[3\left(1-\tfrac{2}{3}Q\right)-1\right]^2\left[(3-2Q)^2-6+4Q-3\right] \\
&= -\left[3\left(1-\tfrac{2}{3}Q\right)-1\right]^2\left[3\left(1-\tfrac{2}{3}Q\right)^2-2\left(1-\tfrac{2}{3}Q\right)-1\right].
\end{aligned} \tag{C6}$$

Finally, we obtain

$$\begin{aligned}
&\tfrac{16}{3}Q(Q-a)(Q-b)(Q-c) + \left[3\left(1-\tfrac{2}{3}Q\right)-1\right]^2 \\
&\times \left[3\left(1-\tfrac{2}{3}Q\right)^2-2\left(1-\tfrac{2}{3}Q\right)-1\right] \geqslant 0.
\end{aligned} \tag{C7}$$

APPENDIX D: SUPPLEMENTARY PROOF OF THE MAXIMUM STEERING INEQUALITY VIOLATION VERSUS CONCURRENCE FILL

1. Proof of Equation (74)

From Eq. (8), we have

$$a \equiv C^2_{A(BC)} = 4\det\rho_A = 4\lambda_1\lambda_2. \tag{D1}$$

Similarly, we find

$$b = 4\lambda_3\lambda_4, \quad c = 4\lambda_5\lambda_6. \tag{D2}$$

Using Eq. (73), we obtain

$$\begin{aligned}
\mathcal{S}_{AB} &= 4\mathrm{Tr}(\rho_C^2) - 2\mathrm{Tr}(\rho_A^2) - 2\mathrm{Tr}(\rho_B^2) + 1 \\
&= 4(\lambda_5^2+\lambda_6^2) - 2(\lambda_1^2+\lambda_2^2) - 2(\lambda_3^2+\lambda_4^2) + 1 \\
&= 4(1-2\lambda_5\lambda_6) - 2(1-2\lambda_1\lambda_2) - 2(1-2\lambda_3\lambda_4) + 1 \\
&= 4\lambda_1\lambda_2 + 4\lambda_3\lambda_4 - 8\lambda_5\lambda_6 + 1 \\
&= a + b - 2c + 1.
\end{aligned} \tag{D3}$$

2. Proof of Equation (77)

Given

$$Q = \tfrac{1}{2}(a+b+c), \tag{D4}$$

where $0 \leqslant a, b, c \leqslant 1$, we obtain $a + b \leqslant 2$. Then, we have

$$4c \leqslant 4 - 2a - 2b + 4c. \tag{D5}$$

This gives

$$2b + 2c - 2a + 2a + 2c - 2b \leqslant 4 - 2(a + b - 2c). \tag{D6}$$

The above equation can be rewritten as

$$\begin{aligned}
&4\left(\frac{a}{2}+\frac{b}{2}+\frac{c}{2}-a\right) + 4\left(\frac{a}{2}+\frac{b}{2}+\frac{c}{2}-b\right) \\
&\leqslant 2[2-(a+b-2c)].
\end{aligned} \tag{D7}$$

Therefore, we obtain

$$4(Q-a) + 4(Q-b) \leqslant 2[2-(a+b-2c)]. \tag{D8}$$

3. Proof of Equation (81)

By using the inequality

$$\begin{aligned}
&4(Q-a)4(Q-b)4(Q-c)4Q \\
&\leqslant [2-(a+b-2c)]^2(2+a+b-2c) \\
&\times [6-(a+b-2c)],
\end{aligned} \tag{D9}$$

we have

$$16^2 Q(Q-a)(Q-b)(Q-c) \leqslant -(a+b-2c-2)^2(a+b-2c+2)(a+b-2c-6) = -(a+b-2c+1-3)^2(a+b-2c+1+1) \times (a+b-2c+1-7). \quad \text{(D10)}$$

Thus, we get

$$48 \times \tfrac{16}{3} Q(Q-a)(Q-b)(Q-c) + (a+b-2c+1-3)^2 \times (a+b-2c+1+1)(a+b-2c+1-7) \leqslant 0. \quad \text{(D11)}$$

APPENDIX E: SUPPLEMENTARY PROOF OF THE MAXIMUM STEERING INEQUALITY VIOLATION VERSUS FIRST-ORDER COHERENCE

1. Proof of Equation (88)

Based on the inequality

$$\mathrm{Tr}(\rho_A^2) + \mathrm{Tr}(\rho_B^2) \geqslant 1, \quad \text{(E1)}$$

we have

$$-6\mathrm{Tr}(\rho_A^2) - 6\mathrm{Tr}(\rho_B^2) + 6 \leqslant 0. \quad \text{(E2)}$$

Then, we can see that

$$4\mathrm{Tr}(\rho_C^2) - 2\mathrm{Tr}(\rho_A^2) - 2\mathrm{Tr}(\rho_B^2) - 4\mathrm{Tr}(\rho_A^2) - 4\mathrm{Tr}(\rho_B^2) - 4\mathrm{Tr}(\rho_C^2) + 6 \leqslant 0. \quad \text{(E3)}$$

Finally, we obtain

$$4\mathrm{Tr}(\rho_C^2) - 2\mathrm{Tr}(\rho_A^2) - 2\mathrm{Tr}(\rho_B^2) + 1 - 6\left\{\tfrac{2}{3}[\mathrm{Tr}(\rho_A^2) + \mathrm{Tr}(\rho_B^2) + \mathrm{Tr}(\rho_C^2)] - 1\right\} \leqslant 1. \quad \text{(E4)}$$

2. Proof of Equation (90)

From the inequality

$$\mathrm{Tr}(\rho_C^2) \leqslant 1, \quad \text{(E5)}$$

we have

$$6\mathrm{Tr}(\rho_C^2) - 2\mathrm{Tr}(\rho_A^2) - 2\mathrm{Tr}(\rho_B^2) + 2\mathrm{Tr}(\rho_A^2) + 2\mathrm{Tr}(\rho_B^2) \leqslant 6. \quad \text{(E6)}$$

Then, we can see that

$$4\mathrm{Tr}(\rho_C^2) - 2\mathrm{Tr}(\rho_A^2) - 2\mathrm{Tr}(\rho_B^2) + 1 + 2\mathrm{Tr}(\rho_A^2) + 2\mathrm{Tr}(\rho_B^2) + 2\mathrm{Tr}(\rho_C^2) - 3 \leqslant 4. \quad \text{(E7)}$$

Finally, we obtain

$$4\mathrm{Tr}(\rho_C^2) - 2\mathrm{Tr}(\rho_A^2) - 2\mathrm{Tr}(\rho_B^2) + 1 + 3\left\{\tfrac{2}{3}[\mathrm{Tr}(\rho_A^2) + \mathrm{Tr}(\rho_B^2) + \mathrm{Tr}(\rho_C^2)] - 1\right\} \leqslant 4. \quad \text{(E8)}$$

[1] A. Einstein, B. Podolsky, and N. Rosen, Phys. Rev. **47**, 777 (1935).
[2] M. A. Nielsen and I. L. Chuang, *Quantum Computation and Quantum Information*, 10th anniversary ed. (Cambridge University Press, Cambridge, 2010).
[3] E. Chitambar and G. Gour, Rev. Mod. Phys. **91**, 025001 (2019).
[4] L. Mandel and E. Wolf, *Optical Coherence and Quantum Optics* (Cambridge University Press, Cambridge, 1995).
[5] K. Bharti, A. Cervera-Lierta, T. H. Kyaw, T. Haug, S. Alperin-Lea, A. Anand, M. Degroote, H. Heimonen, J. S. Kottmann, T. Menke, W.-K. Mok, S. Sim, L.-C. Kwek, and A. Aspuru-Guzik, Rev. Mod. Phys. **94**, 015004 (2022).
[6] V. Giovannetti, S. Lloyd, and L. Maccone, Nat. Photonics **5**, 222 (2011).
[7] Z.-H. Ma, J. Cui, Z. Cao, S.-M. Fei, V. Vedral, T. Byrnes, and C. Radhakrishnan, Europhys. Lett. **125**, 50005 (2019).
[8] R. Horodecki, P. Horodecki, and M. Horodecki, Phys. Lett. A **200**, 340 (1995).
[9] W. K. Wootters, Phys. Rev. Lett. **80**, 2245 (1998).
[10] J. Eisert and M. B. Plenio, J. Mod. Opt. **46**, 145 (1999).
[11] A. Sen(De) and U. Sen, Phys. Rev. A **81**, 012308 (2010).
[12] T. Das, S. S. Roy, S. Bagchi, A. Misra, A. Sen(De), and U. Sen, Phys. Rev. A **94**, 022336 (2016).
[13] D. Sadhukhan, S. S. Roy, A. K. Pal, D. Rakshit, A. Sen(De), and U. Sen, Phys. Rev. A **95**, 022301 (2017).
[14] T.-C. Wei and P. M. Goldbart, Phys. Rev. A **68**, 042307 (2003).
[15] Z.-H. Ma, Z.-H. Chen, J.-L. Chen, C. Spengler, A. Gabriel, and M. Huber, Phys. Rev. A **83**, 062325 (2011).
[16] S. M. Hashemi Rafsanjani, M. Huber, C. J. Broadbent, and J. H. Eberly, Phys. Rev. A **86**, 062303 (2012).
[17] S. Xie and J. H. Eberly, Phys. Rev. Lett. **127**, 040403 (2021).
[18] E. Schrödinger, Proc. Cambridge Philos. Soc. **31**, 555 (1935).
[19] E. G. Cavalcanti, S. J. Jones, H. M. Wiseman, and M. D. Reid, Phys. Rev. A **80**, 032112 (2009).
[20] A. C. S. Costa and R. M. Angelo, Phys. Rev. A **93**, 020103(R) (2016).
[21] M. Żukowski, A. Dutta, and Z. Yin, Phys. Rev. A **91**, 032107 (2015).
[22] S. P. Walborn, A. Salles, R. M. Gomes, F. Toscano, and P. H. Souto Ribeiro, Phys. Rev. Lett. **106**, 130402 (2011).
[23] J. Schneeloch, C. J. Broadbent, S. P. Walborn, E. G. Cavalcanti, and J. C. Howell, Phys. Rev. A **87**, 062103 (2013).
[24] T. Kriváchy, F. Fröwis, and N. Brunner, Phys. Rev. A **98**, 062111 (2018).
[25] D. Wang, F. Ming, M.-L. Hu, and L. Ye, Ann. Phys. (Berlin, Ger.) **531**, 1900124 (2019).
[26] S. Wollmann, R. Uola, and A. C. S. Costa, Phys. Rev. Lett. **125**, 020404 (2020).
[27] Y. Yao, X. Xiao, L. Ge, and C. P. Sun, Phys. Rev. A **92**, 022112 (2015).
[28] D. E. Bruschi, C. Sabín, and G. S. Paraoanu, Phys. Rev. A **95**, 062324 (2017).

[29] K. C. Tan, S. Choi, H. Kwon, and H. Jeong, Phys. Rev. A **97**, 052304 (2018).
[30] X. Yuan, H. Zhou, M. Gu, and X. Ma, Phys. Rev. A **97**, 012331 (2018).
[31] F. Ming, D. Wang, L.-J. Li, X.-G. Fan, X.-K. Song, L. Ye, and J.-L. Chen, Adv. Quantum Technol. **4**, 2100036 (2021).
[32] W. Vogel and J. Sperling, Phys. Rev. A **89**, 052302 (2014).
[33] J. K. Asbóth, J. Calsamiglia, and H. Ritsch, Phys. Rev. Lett. **94**, 173602 (2005).
[34] H. Yang, Z.-Y. Ding, X.-K. Song, H. Yuan, D. Wang, J. Yang, C.-J. Zhang, and L. Ye, Phys. Rev. A **103**, 022207 (2021).
[35] U. Singh, M. N. Bera, H. S. Dhar, and A. K. Pati, Phys. Rev. A **91**, 052115 (2015).
[36] K. H. Kagalwala, G. Di Giuseppe, A. F. Abouraddy, and B. E. Saleh, Nat. Photonics **7**, 72 (2013).
[37] J. Svozilík, A. Vallés, J. Peřina, and J. P. Torres, Phys. Rev. Lett. **115**, 220501 (2015).
[38] A. Streltsov, U. Singh, H. S. Dhar, M. N. Bera, and G. Adesso, Phys. Rev. Lett. **115**, 020403 (2015).
[39] A. Černoch, K. Bartkiewicz, K. Lemr, and J. Soubusta, Phys. Rev. A **97**, 042305 (2018).
[40] X.-G. Fan, W.-Y. Sun, Z.-Y. Ding, F. Ming, H. Yang, D. Wang, and L. Ye, New J. Phys. **21**, 093053 (2019).
[41] J. K. Kalaga, W. Leoński, and J. Peřina, Phys. Rev. A **97**, 042110 (2018).
[42] M. T. Quintino, T. Vértesi, D. Cavalcanti, R. Augusiak, M. Demianowicz, A. Acín, and N. Brunner, Phys. Rev. A **92**, 032107 (2015).
[43] Y. Z. Law, L. P. Thinh, J.-D. Bancal, and V. Scarani, J. Phys. A **47**, 424028 (2014).
[44] M. Piani and J. Watrous, Phys. Rev. Lett. **114**, 060404 (2015).
[45] C. Branciard and N. Gisin, Phys. Rev. Lett. **107**, 020401 (2011).
[46] C. Branciard, E. G. Cavalcanti, S. P. Walborn, V. Scarani, and H. M. Wiseman, Phys. Rev. A **85**, 010301(R) (2012).
[47] M.-M. Du and D. M. Tong, Phys. Rev. A **103**, 032407 (2021).
[48] Z.-Y. Ding, P.-F. Zhou, J.-X. Liu, C.-C. Liu, M. Zhao, H. Yang, X.-G. Fan, J. He, and L. Ye, Opt. Express **29**, 40668 (2021).
[49] A. Kumar and H. S. Dhar, Phys. Rev. A **93**, 062337 (2016).
[50] A. Kumar, H. S. Dhar, R. Prabhu, A. Sen(De), and U. Sen, Phys. Lett. A **381**, 1701 (2017).
[51] T. Pramanik, Y.-W. Cho, S.-W. Han, S.-Y. Lee, Y.-S. Kim, and S. Moon, Phys. Rev. A **99**, 030101(R) (2019).
[52] B. Paul and K. Mukherjee, Phys. Rev. A **102**, 052209 (2020).
[53] T.-Z. Dai, Y. Fan, and L. Qiu, Phys. Rev. A **105**, 022425 (2022).
[54] Y. Pu, Y. Wu, N. Jiang, W. Chang, C. Li, S. Zhang, and L. Duan, Sci. Adv. **4**, eaar3931 (2018).
[55] N. Friis, O. Marty, C. Maier, C. Hempel, M. Holzäpfel, P. Jurcevic, M. B. Plenio, M. Huber, C. Roos, R. Blatt, and B. Lanyon, Phys. Rev. X **8**, 021012 (2018).
[56] V. Saggio, A. Dimić, C. Greganti, L. A. Rozema, P. Walther, and B. Dakić, Nat. Phys. **15**, 935 (2019).
[57] D. A. Meyer and N. R. Wallach, J. Math. Phys. **43**, 4273 (2002).
[58] G. K. Brennen, Quantum Inf. Comput. **3**, 619 (2003).
[59] V. Coffman, J. Kundu, and W. K. Wootters, Phys. Rev. A **61**, 052306 (2000).
[60] I. Bengtsson and K. Życzkowski, *Geometry of Quantum States: An Introduction to Quantum Entanglement*, 2nd ed. (Cambridge University Press, Cambridge, 2017); K. Zyczkowski and M. Kus, J. Phys. A **27**, 4235 (1994).
[61] P. Pandya, A. Misra, and I. Chakrabarty, Phys. Rev. A **94**, 052126 (2016).
[62] R. Nepal, R. Prabhu, A. Sen(De), and U. Sen, Phys. Rev. A **87**, 032336 (2013).
[63] S. Boyd and L. Vandenberghe, *Convex Optimization* (Cambridge University Press, Cambridge, 2004).